

Confidence-Aware Deep Learning for Load Plan Adjustments in the Parcel Service Industry

Thomas Bruys Reza Zandehshahvar Amira Hijazi Pascal Van Hentenryck
NSF Artificial Intelligence Research Institute for Advances in Optimization, Atlanta, USA
Georgia Institute of Technology, Atlanta, USA
{thomas.bruys, ahijazi6}@gatech.edu
{reza, pascal.vanhentenryck}@isye.gatech.edu

Abstract

This study develops a deep learning-based approach to automate inbound load plan adjustments for a large transportation and logistics company. It addresses a critical challenge for the efficient and resilient planning of E-commerce operations in presence of increasing uncertainties. The paper introduces an innovative data-driven approach to inbound load planning. Leveraging extensive historical data, the paper presents a two-stage decision-making process using deep learning and conformal prediction to provide scalable, accurate, and confidence-aware solutions. The first stage of the prediction is dedicated to tactical load-planning, while the second stage is dedicated to the operational planning, incorporating the latest available data to refine the decisions at the finest granularity. Extensive experiments compare traditional machine learning models and deep learning methods. They highlight the importance and effectiveness of the embedding layers for enhancing the performance of deep learning models. Furthermore, the results emphasize the efficacy of conformal prediction to provide confidence-aware prediction sets. The findings suggest that data-driven methods can substantially improve decision making in inbound load planning, offering planners a comprehensive, trustworthy, and real-time framework to make decisions. The initial deployment in the industry setting indicates a high accuracy of the proposed framework.

1 Introduction

In recent decades, the trucking industry has experienced significant changes driven by the rapid growth of E-commerce, driven by increased online shopping and reduced reliance on physical stores, thereby altering logistics and delivery demands. According to the American Trucking Association, in 2022, 72% of total US domestic tonnage was shipped via trucks, which corresponds to 11.46 billion tons of freight (Associations 2023). This represents a significant increase over the past ten years, up from 8.19 billion tons in 2012 (U.S. Department of Transportation 2014). This dramatic surge in demand has profoundly impacted parcel service industries, creating an urgent need for advanced logistics capabilities to efficiently plan and manage shipments across

large-scale logistics networks, while meeting customer expectations.

Load planning is crucial to the operations of these logistic networks, as it defines the transportation capacity of the network (Bakir, Erera, and Savelsbergh 2021). At the tactical level, e.g., a week before the day of operations, load planning determines the number of trailers to allocate across the network to serve the forecasted demand. Tactical planning typically uses average estimates for demand. However, actual demand can vary significantly, rendering the tactical plan less effective on the day of operations (Lindsey, Erera, and Savelsbergh 2016). To address this challenge, parcel service companies adjust their tactical plans on the day of operations by re-routing shipments on alternative paths, modifying the arrivals and due times of some shipments, or shifting inbound loads (Crainic 2000a).

This paper is motivated by the need of an industry partner, one of the largest parcel shipment companies, for a decision-support tool to automate inbound load-shifting process. Load shifting is the process of re-directing inbound loads to a different destination. Currently, these decisions are being made manually, requiring planners to evaluate both load-specific and destination-specific data to make quick decisions about where to process each load. To alleviate the burden on human planners, this paper proposes a machine learning (ML) decision-support tool to predict the processing building and sort of each planned load (i.e., the location and time that the loads are planned to be processed). The proposed model acts as a proxy for the automation of load-shifting decision-making which enables faster, more consistent, and reliable decisions, while reducing the burden on human planners. Moreover, the machine learning tool can learn from both historical decisions made by human planners and optimal decisions generated by optimization programs, allowing for both high-quality decisions and real-time decision support.

The key contribution of the paper is a two-stage decision-support framework, that captures the needs of both tactical and operational load planning. At the tactical level (stage 1), one week prior to the day of operation, the model predicts the building and sort for each load. This allows planners to anticipate potential load shifts in advance and thus enables efficient resource allocation. At the operational level (stage 2), the model provides real-time adaptability on the

This research was supported by NSF award 2112533

day of operation by refining sort predictions based on updated forecasts, such as the estimated arrival time of each load. Attempting to refine the building prediction on the day of operations is not feasible, as it would create delays and violate service commitments. *The proposed two-stage framework effectively balances the need for proactive planning with the flexibility to adapt to real-time conditions.*

A key aspect of the approach is to integrate training data from buildings across multiple clusters, enriching the decision-support tool with a network-wide perspective based on the features of the planned destinations. This ensures that *decisions at the building level are informed by a comprehensive understanding of the entire network*, leading to more effective load planning.

The framework also incorporates conformal prediction to provide confidence-aware recommendations. Relying on single-point predictions can lead to disruptions in the downstream logistics process if these predictions are incorrect, reducing the trustworthiness of the ML model. Conformal prediction addresses this issue by providing a prediction set with theoretical guarantees, ensuring that the true processing location and sort are included within the recommendations with a specified confidence level.

1.1 Related Work

Load Planning

This paper contributes to the literature on service network design for freight transportation, specifically focusing on load planning. While load planning at the tactical level has been widely studied, there has been less emphasis on operational planning.

Tactical load planning involves determining the number of trailers to dispatch between each pair of terminals as well as the time of dispatch. (Boland et al. 2017) modeled this problem as a space-time network and proposed an iterative refinement algorithm based on dynamic discretization discovery (DDD). (Hewitt 2019) enhanced DDD by using acceleration techniques, including relaxations, valid inequalities, and symmetry breaking. For comprehensive survey on tactical load planning, the readers are referred to (Crainic 2000b), (Wieberneit 2007), and (James C. Chen and Chen 2024).

Operational planning involves the adjustment of the tactical plan by re-routing shipments on alternative paths, modifying the arrivals and due times of some shipments, or shifting inbound loads to hedge against day-to-day demand changes and operational constraints (Crainic 2000a). The value of re-routing shipments on p alternative paths is highlighted in (Baubaid, Boland, and Savelsbergh 2018). Building on this, (Herszterg et al. 2022) proposed a near real-time solution for operational planning that effectively considers one alternative path. More recently, (Ojha et al. 2024) developed an ML proxy for dynamic outbound load plans, enabling the operational load plan to be adjusted dynamically as package volumes change.

The aforementioned studies primarily addressed outbound decision-making. On the inbound side, (McWilliams 2009) introduced a framework for optimizing unload schedules of the inbound loads to minimize the time-span of trans-

fer operations using a dynamic load-balancing algorithm. Additionally, (Bugow and Kellenbrink 2023) employed a genetic algorithm to optimize inbound truck scheduling.

ML in Parcel Service Industry

In recent years, the increasing availability of data has driven the popularity of applying ML methods across various domains. To date, ML has primarily been applied in the parcel service industry for arrival time estimation, demand forecasting, vehicle routing, and containerization, as discussed in the survey by (Tsolaki et al. 2023). For example, (Munkhdalai et al. 2020) presented a Deep Learning (DL) approach for demand forecasting in the parcel service industry during special holidays, while (Ye et al. 2024) proposed a graph-learning based method coupled with a temporal attention module for inbound parcel volume forecasting. (Eskandarzadeh and Fahimnia 2024) demonstrate a hybrid ML and optimization approach for parcel sortation and containerisation decisions.

Although ML methods hold considerable potential, their practical deployment often faces challenges, such as insufficient trust and inconsistent reliability. ML models can sometimes make incorrect decisions with high confidence, compounding these concerns. This paper addresses these issues by leveraging conformal prediction, which is a distribution-free and model-agnostic approach (Vovk, Gammerman, and Shafer 2005; Romano, Sesia, and Candès 2020; Angelopoulos et al. 2022). Within the context of parcel service industry, conformal prediction has been utilized for uncertainty quantification of the time and location of pick-up requests made by customers to couriers (Yan et al. 2024). However, this is still an under-explored area of research in the parcel service industry.

1.2 Contributions

To the best of our knowledge, this paper is the first to introduce a confidence-aware data-driven framework to facilitate fast, reliable, and scalable inbound decision making for both tactical and operational load planning. More precisely, for each load, the proposed approach predicts the inbound destination of each load by utilizing a two-stage decision-making framework. The first stage takes place one week before the day of operations and predicts the building and sort for processing each load. This tactical-level prediction is crucial as it allows planners to identify loads that must be shifted to different buildings well in advance, enabling the proper resource allocation. The second stage takes place on the day of operations and refines the sort prediction based on updated forecasts, including the estimated arrival time of each load. The two-stage approach is motivated by the lack of reliable data on the planned arrival time of the loads a week before operations, which limits the performance of the single-stage approach in predicting sorts.

The main contributions of the paper can be summarized as follows.

1. The paper develops a deep-learning method tailored for tabular data to automate load plan adjustments in parcel service industry. The method obtains reliable predictions through a two-stage decision-making process,

which captures both planning and operational constraints and objectives.

2. The proposed framework returns confidence-aware solutions by enhancing the two-stage method with conformal prediction. This allows planners to focus on the less confident predictions, enhancing the overall robustness of the decision-making process and reducing their cognitive burden.
3. The paper validates the proposed framework using an industrial dataset collected over 1.5 years and consisting of more than 250,000 loads. The results demonstrate that buildings and sorts can be predicted with an overall accuracy of 99% and 87%, respectively, one week before the day of operations. The second stage, with the refinement of the sort prediction on the day of operations, allows an improvement of 5% in overall accuracy, and 20% on the shifted loads, compared to forecasts made a week prior. Additionally, the conformal prediction results demonstrate that the proposed method provides reliable and typically small prediction sets, while reaching the target coverage rate.

1.3 Structure of the Paper

The remainder of the paper is organized as follows. Section 2 presents the problem of inbound load planning considered in this paper. Section 3 reviews the data provided by the industrial partner. Section 4 presents the architecture of the proposed DL-based and confidence-aware framework. Section 5 describes the case study and experiments. The results and comparisons of different methods including traditional ML models and DL architectures are discussed in Section 6 followed by the conclusions in Section 7.

2 Problem Statement

Table 1 presents the nomenclature and defines all symbols and notations used throughout the paper. Logistic networks are organized into clusters of *buildings*, defined either geographically or based on the frequency of interactions between buildings. Within these networks, outbound trailers, also referred to as *loads*, from upstream buildings are planned to arrive and be processed at downstream buildings during specific time windows, known as *sorts*, which divide a typical operational day into three periods: S1, S2, and S3.

Consider a set of inbound loads \mathcal{L} that are planned to be sorted at building b'_l and sort s'_l . Human planners at a building $b'_l \in \mathcal{B}$ within a cluster $g \in \mathcal{G}$ evaluate the operational status of their terminal and, based on their expertise and real-time changes, decide which loads need to be shifted to different buildings or sorts. This evaluation is guided by both load-level features, such as the origin, planned volume, and planned arrival time, and building-level features, including the planned work staff and planned volume to be processed during each sort. A load is considered shifted when its *actual processing building* b_l , or *actual processing sort* s_l differs from the planned processing location, i.e. $(b_l, s_l) \neq (b'_l, s'_l)$. There are two types of shifts:

- **Internal shifts:** These occur when the actual processing building is the same as the planned processing building

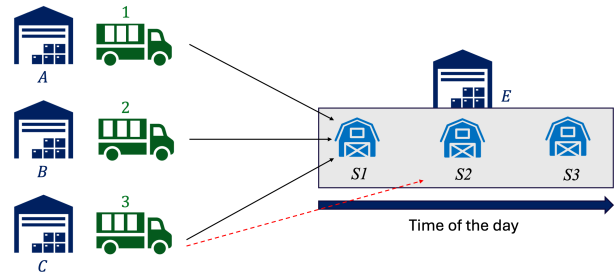


Figure 1: Illustration of an internal shift, where load 3 was planned to be processed during sort $S1$ in building E but was actually processed during sort $S2$ in building E .

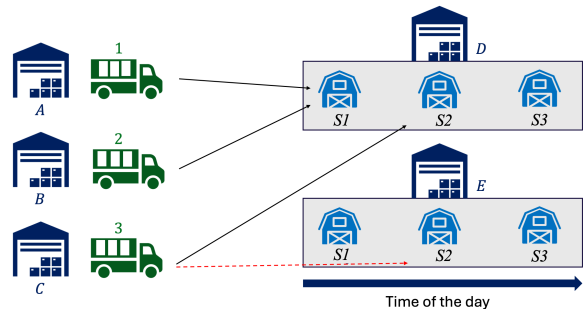


Figure 2: Illustration of an external shift, where load 3 was planned to be processed during sort $S2$ in building D but was actually processed during sort $S2$ in building E .

for load l , but the actual processing sort, denoted by s_l , differs from the planned processing sort, denoted by s'_l (i.e., $b'_l = b_l$ and $s'_l \neq s_l$).

- **External shifts:** These occur when the actual processing building of load l , denoted by b_l , is different from the planned processing building, denoted by b'_l (i.e., $b'_l \neq b_l$).

Figure 1 presents an internal shift, where load 3, with planned processing building $b'_3 = E$ and planned processing sort $s'_3 = D$, is processed in the planned building (i.e., $b'_3 = b_3 = E$), but at a different sort $s_3 = T$. Similarly, Figure 2 depicts an external shift for load 3, where the load is redirected from the planned processing building $b'_3 = E$ to $b_3 = F$. Note that the actual processing sort for external shifts may be the same or differ from the planned sort.

Given a set of loads \mathcal{L} and their associated feature vectors \mathbf{X} , which includes both load-level and building-level features for the planned processing building, the objective is to provide a data-driven decision-support tool to predict the processing building and sort for each planned load (i.e., b_l and s_l for $l \in \mathcal{L}$, with predictions denoted as $\hat{y}_{b,w}$ for building and $\hat{y}_{s,w}$ and $\hat{y}_{s,d}$ for sort. Here, the subscript w refers to the predictions made one week prior to the day of operations while the subscript d corresponds to the predictions made on the day of operations). This paper develops a confidence-aware prediction method to reduce the cognitive burden of planners and operators in tactical and operational settings.

Table 1: Nomenclature

Sets	Description
\mathcal{L}	The set of loads (i.e., aggregation of shipments that share the same origin, destination and due date).
\mathcal{B}	The set of buildings.
\mathcal{S}	The set of sorts, defined based on the processing times of the loads (e.g., S1, S2, and S3.)
\mathcal{G}	The set of building clusters (i.e., aggregation of buildings within the same state).
Parameters	Description
$l \in \mathcal{L}$	Load identifier.
$b'_l \in \mathcal{B}$	Planned processing building of load l .
$b_l \in \mathcal{B}$	Actual processing building of load l .
$s'_l \in \mathcal{S}$	Planned processing sort of load l .
$s_l \in \mathcal{S}$	Actual processing sort of load l .
ML Nomenclature	Description
\mathbf{X}	Input data corresponding to a set of features.
\mathcal{D}_{train}	Training Set.
$\mathcal{D}_{validation}$	Validation Set.
$\mathcal{D}_{calibration}$	Calibration Set.
$\mathcal{D}_{testing}$	Testing Set.
y_b	Target processing building.
y_s	Target processing sort.
$\hat{y}_{b,w}$	Predicted processing building a week prior the day of operations.
$\hat{y}_{s,w}$	Predicted processing sort a week prior the day of operations.
$\hat{y}_{s,d}$	Predicted processing sort on the day of operations.
$\hat{y}_{b,w}^{cp}$	Conformalized prediction set of buildings a week prior the day of operations.
$\hat{y}_{s,w}^{cp}$	Conformalized prediction set of sorts a week prior the day of operations.
$\hat{y}_{s,d}^{cp}$	Conformalized prediction set of sorts on the day of operations.

3 Data Overview

This section reviews the data available for decision support.

3.1 Data Description

This research utilized historical data from the industrial partner. The dataset consists of 250,000 planned loads, with origins and destinations spanning two clusters across two states and three distinct sorts (i.e., $|\mathcal{G}| = 2$, $|\mathcal{B}| = 6$, and $|\mathcal{S}| = 3$), collected between September 2022 and January 2024.

The dataset comprises two levels of information essential for accurate prediction: 1) load-level data and 2) building-level data. Load-level data contains detailed information for each planned load, including origin, planned destination, planned volume, and estimated arrival time. Each load is associated with a planned processing building and sort, as well as the actual building and sort where it was processed. The

building-level data is associated with the planned processing building on the estimated arrival date. It includes building-level features such as the number of packages scheduled to be processed at the location, along with the planned workforce.

The dataset features are categorized into temporal, numerical, and categorical types. After their encoding (described in Section 5.1), temporal features are treated as numerical and are referred to as such hereafter. The temporal and numerical features are described together in Table 2, and the categorical features are detailed in Table 3. The estimated arrival time of the loads at the processing facility is a crucial feature, which is used exclusively for predictions on the day of operation (i.e., stage 2).

The dataset is first sorted based on estimated arrival times due to its temporal nature. It is then divided into training, validation, calibration, and testing sets (see Section 5.2 for further details). The training set is used to tune the model,

Table 2: Description of the numerical features. The planned values refer to the operations expected to be performed at the planned processing building and sort (b'_l, s'_l) on the estimated arrival date of load l .

Feature	Description
Pln Volume	Volume planned to be processed
Pln PPH	Planned packages processed per hour
Pln payroll	Planned total staffing on payroll
Pln work staff	Planned number of employees working
Pln runtime	Planned total operation run time
Pln process rate	Planned number of packages scanned per hour
Pln FPH	Planned number of unloaded and sorted packages
Pln unload span	Planned time unload will operate
Load volume	Volume of the considered load
Load creation date	Creation date of the load in its origin location
Est Arr date	Estimated Arrival date of the load
Est Arr Time	Estimated Arrival time of the load (used for predictions in operational settings)

Table 3: Description of the categorical features

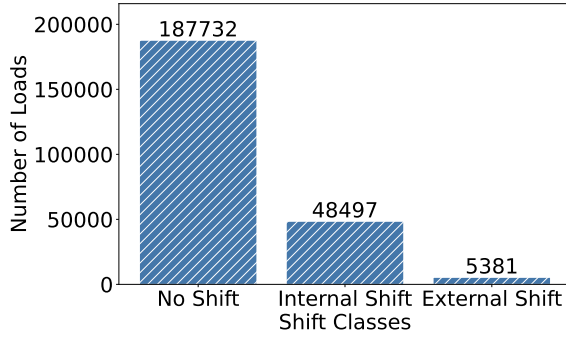
Feature	Description	Unique Values
Pln dest cluster	Planned destination cluster of the load	2
Pln dest building (b'_l)	Planned processing building of the load	6
Pln dest sort (s'_l)	Planned processing sort of the load	3
Org building	Origin building of the load	329
Org sort	Origin sort of the load	8

while the validation set helps identify the optimal hyperparameters. The calibration set is specifically reserved for uncertainty quantification through conformal prediction. The test set is used for evaluation of the model performance. The specifics of the models and conformal prediction are detailed in Section 4 followed by the experimental details in Section 5.

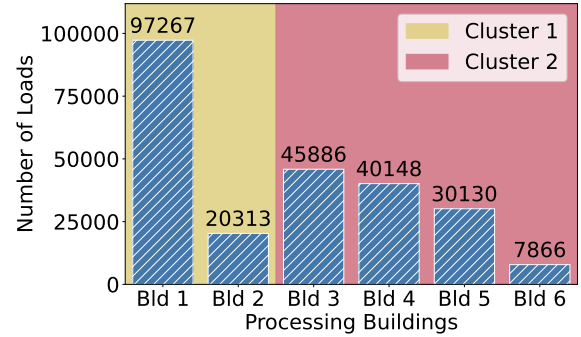
3.2 Data Analysis

Figure 3 presents the distribution of loads across several dimensions. Figure 3(a) shows that the data contains significant class imbalance among different shift classes with majority of the loads coming from the "No Shift" class, meaning that the planned processing location is same as the processing location. *A crucial challenge addressed by the proposed framework is to identify shifted loads without gener-*

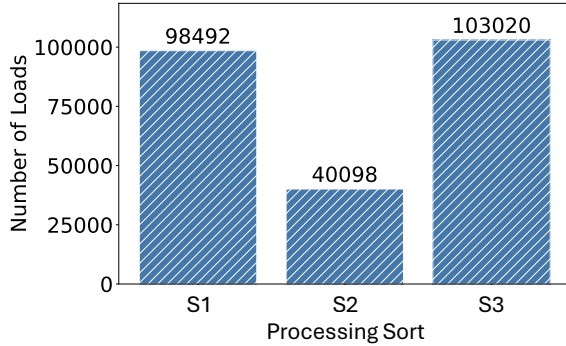
ating excessive false alarms, i.e., predicting shifts for loads that should not be shifted. Furthermore, Figures 3(b) and 3(c) demonstrate that the distribution of loads across different buildings and sorts is not uniform. Specifically, Building 1 from Cluster 1 processes around 41% of the loads, while the second most active building processes approximately half as many. Regarding sorts, S2 processes only around 17% of the loads, while the rest of the loads is uniformly processed by S1 and S3 sorts. Additionally, Figure 3(d) reveals that the network is almost inactive during weekends. *The imbalance and complexity of the data underscore the need for a unified decision-making tool that leverages historical data from the whole network to make informed decisions.*



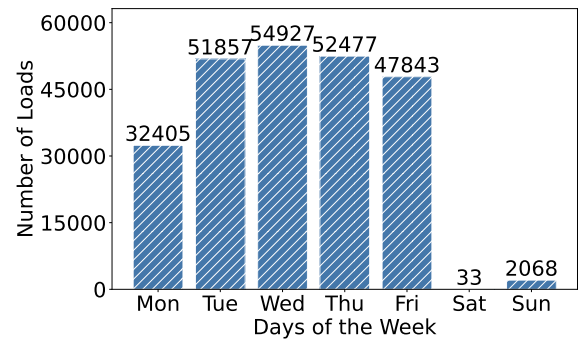
(a) Number of loads per shift class



(b) Number of loads per building



(c) Number of loads per sort



(d) Number of loads per day of the week

Figure 3: Number of loads through different dimensions: (a) The number of loads per shift class. (b) The number of loads processed in different buildings. (c) The number of loads processed in each sort. (d) The number of loads processed during each day of the week.

4 The Machine Learning Framework

Consider a set of loads \mathcal{L} and their corresponding input features \mathbf{X} , which consists of a set of numerical and categorical features, i.e., $\mathbf{X} = (\mathbf{X}^{cont}, \mathbf{X}^{cat})$, as outlined in Tables 2 and 3. The goal is to make predictions for each load $l \in \mathcal{L}$ at two time points: 1) the building and sort one week before the day of the operation and 2) predicting the sort on the day of operation, given additional features that became available. Therefore, the three target prediction tasks can be formalized as follows:

Stage 1: Week ahead prediction:

- $\mathbf{f}_{b,w} : \mathbf{X}_{b,w} \rightarrow y_b$, where $\mathbf{X}_{b,w} \subseteq \mathbf{X}$ is the set of features available one week before the day of operations for the building prediction.
- $\mathbf{f}_{s,w} : \mathbf{X}_{s,w} \rightarrow y_s$, where $\mathbf{X}_{s,w} \subseteq \mathbf{X}$ corresponds to $\mathbf{X}_{b,w}$ enriched with y_b during training and \hat{y}_b during inference.

Stage 2: Day of operation prediction:

- $\mathbf{f}_{s,d} : \mathbf{X}_{s,d} \rightarrow y_s$, where $\mathbf{X}_{s,d} \subseteq \mathbf{X}$ corresponds to $\mathbf{X}_{s,w}$ enriched with the estimated arrival times of the loads.

As discussed in Section 2, the motivation behind the two-step decision-making process is to predict the buildings and

sorts for the tactical planning, and use the most recent status of the loads to predict the sorts on the day of operation and adjust to the uncertainties in the network for operational planning. Each one of these mappings is learned through supervised empirical risk minimization. By omitting the subscripts (for simplicity and without loss of generality), the learning problems can be formalized as:

$$\min_{\theta} \mathbb{E}_{(\mathbf{X}, y) \sim P_{\mathcal{D}}} [L(\mathbf{f}(\mathbf{X}, \theta), y)], \quad (1)$$

where θ is the vector of model parameters, $P_{\mathcal{D}}$ is the data distribution, and L is the loss function (e.g., categorical cross entropy loss). Since the true data distribution $P_{\mathcal{D}}$ is usually unknown, empirical risk minimization (ERM) is performed to find the model parameters, using N pairs of training data $\mathcal{D}_{\text{train}}$, where $N = |\mathcal{D}_{\text{train}}|$.

Figure 4 shows the schematic of the proposed DL architecture. During the training process, the building prediction model $\mathbf{f}_{b,w}$ takes as input the feature vector $\mathbf{X}_{b,w}$, which corresponds to the features available a week before the day of operation. Next, the numerical and categorical features are mapped into a new vector space through dedicated embedding layers to capture the complex and nonlinear relations in the structured data. The resulting data is then passed into the Neural Network (NN) (e.g., multi-layer perceptron (MLP)

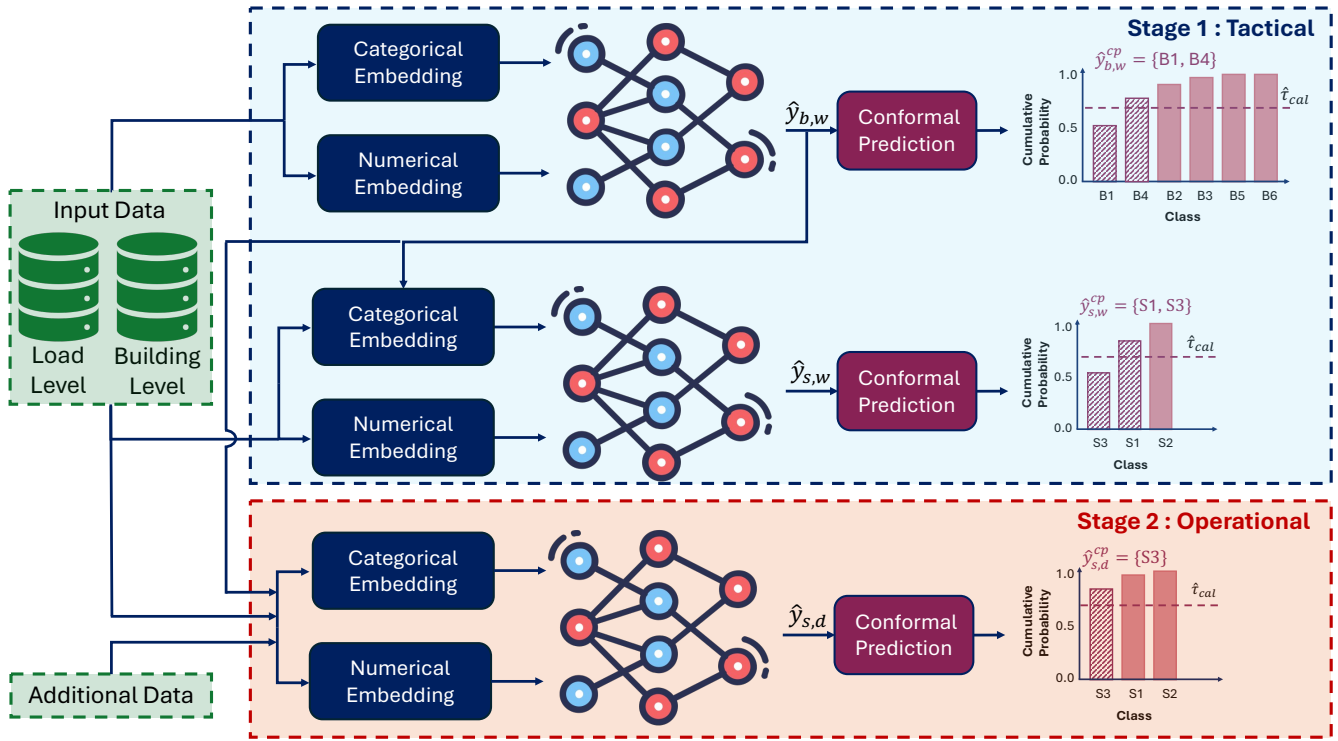


Figure 4: The Framework description. First, the data is embedded through dedicated layers for categorical and numerical features respectively. Then, a neural network predicts the building of the load. This prediction is used as an input feature for the sort prediction, which has a similar architecture. The sort prediction is refined with additional information on the day of operations (i.e., Stage 2). Conformal prediction is performed for both building and sort predictions to provide prediction sets with a pre-specified confidence level. The figure illustrates the cumulative probabilities with classes ordered in decreasing order of estimated probabilities.

or Residual Network (ResNet)) and the model parameters are optimized by minimizing the categorical cross entropy loss. The tactical-level sort prediction model $f_{s,w}$ uses input features similar to the building prediction model but also includes the actual processing buildings as an additional feature (i.e., $\mathbf{X}_{s,w}$), which is essential for accurate sort predictions. Finally, the sort prediction model for the day of operation, i.e., $f_{s,d}$ is trained using the same input features as model $f_{s,w}$ plus the estimated arrival time of the loads as an additional feature (i.e., $\mathbf{X}_{s,d}$). Each of these models is trained using the same training dataset $\mathcal{D}_{\text{train}}$ and the hyperparameters are tuned using a validation dataset $\mathcal{D}_{\text{validation}}$. A calibration dataset $\mathcal{D}_{\text{calibration}}$ is used for conformal prediction, to provide a prediction set that guarantees to include the correct label with a pre-defined confidence level.

At inference time, the processing building is first predicted as $\hat{f}_{b,w}(\mathbf{X}_{b,w}) = \hat{y}_{b,w}$ along with the conformalized prediction set $\hat{y}_{b,w}^{cp}$. Next, the predicted building $\hat{y}_{b,w}$ (i.e., output class of the softmax with the highest probability) is concatenated with the feature vectors and is used as an input to the week-ahead sort prediction model to predict the processing sort as $\hat{f}_{s,w}(\mathbf{X}_{s,w}) = \hat{y}_{s,w}$ and the prediction set $\hat{y}_{s,w}^{cp}$. Finally, on the day of operation, the trained model $f_{s,d}$ takes as input the feature vectors $\mathbf{X}_{s,d}$ concatenated with

the building prediction $\hat{y}_{b,w}$ and the estimated arrival time of the load as additional features to predict the final processing sort as $\hat{y}_{s,d}$ and the prediction set $\hat{y}_{s,d}^{cp}$. Sections 4.1 and 4.2 provide further details on the embedding layers and the conformal prediction model.

4.1 Feature Embedding

Embeddings play a crucial role in enhancing the performance of DL models over tabular and unstructured data as they allow models to more effectively capture the underlying relationships within the data (Gorishniy, Rubachev, and Babenko 2023). The proposed framework employs dedicated embeddings to handle categorical and numerical features separately.

Categorical Embeddings

A powerful technique for embedding categorical features, which is mainly popular within natural language processing domain for generation of word embeddings, amounts to creating a trainable look-up table that maps each unique value of a categorical feature to an n -dimensional vector (Mikolov et al. 2013). The process begins by initializing the look-up table randomly. The entries are then adjusted iteratively through backpropagation to optimize the embeddings. Figure 5 shows a simple example of a look-up table for a cate-

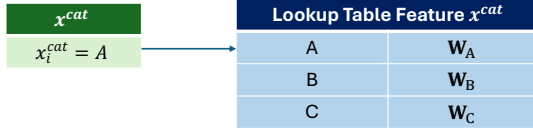


Figure 5: Categorical Embeddings: Value $x_i^{cat} = A$ of feature x^{cat} for sample i is embedded as vector W_A using the Look-up table of the corresponding feature.

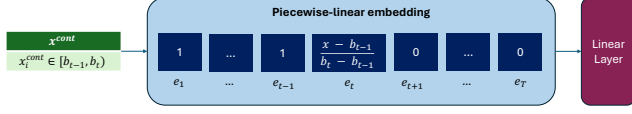


Figure 6: QL Embeddings : Quantile-based bins are created based on the distribution of the values of the numerical features. Then, values are encoded individually based on the the bin they are in. A linear layer is added after the encoding step.

gorical feature.

Consider a categorical feature $x^{cat} \in \mathbf{X}^{cat}$ with C unique values. Each unique value u of x^{cat} is mapped to a n -dimensional vector \mathbf{W}_u , forming a $(C \times n)$ look-up table, where C represents the cardinality of the feature. In this paper, the embedding vector dimension n can be specified as:

$$n = \min(n_{max}, \frac{C + 1}{2}), \quad (2)$$

where $n_{max} = 50$ is the maximum size of the embedding for the categorical features. This embedding approach allows the model to learn dense vector representations of categorical variables, capturing complex relationships that enhance performance in downstream tasks. The embeddings are trained separately for building and sort prediction, as shown in Figure 4.

Numerical Embeddings

Embedding numerical features can also enhance the performance and robustness of DL models significantly on tabular datasets (Gorishniy, Rubachev, and Babenko 2023). Specifically, Gorishniy et al. introduced two embedding techniques: Quantile-based Piecewise-Linear Embeddings (QL) and Periodic Linear Embeddings (PLR). Both methods have demonstrated strong performance, as reported by (Gorishniy, Rubachev, and Babenko 2023), and extensive experiments have been performed to evaluate their performance in this paper.

• QL Embedding

Given a numerical feature $x^{cont} \in \mathbf{X}^{cont}$, this feature is mapped into a T -dimensional vector as illustrated in Figure 6. Formally, for a sample data point i , the embeddings are defined as follows :

$$\mathbf{z}_i = f(x_i^{cont}) = \text{Linear}(\text{PLE}(x_i^{cont})), \quad (3)$$

where :

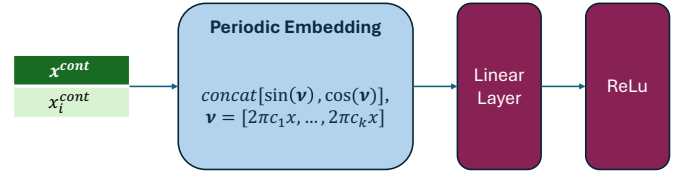


Figure 7: PLR Embeddings : Numerical features are first embedded using periodic embeddings. Then, a linear layer and ReLU activation functions are applied to the output.

$$PLE(x) = [e_1, \dots, e_T] \in \mathbb{R}^T,$$

$$e_t = \begin{cases} 0 & \text{if } x < b_{t-1} \text{ and } t > 1, \\ 1 & \text{if } x \geq b_t \text{ and } t < T, \\ \frac{x - b_{t-1}}{b_t - b_{t-1}} & \text{otherwise,} \end{cases} \quad (4)$$

and $[b_{t-1}; b_t)$ are bins obtained from empirical quantiles for each individual feature. For feature $x^{cont} \in \mathbf{X}^{cont}$, $b_t = Q_{\frac{t}{T}}(\{x_i^{cont}\}_{i \in \mathcal{D}_{train}})$ where $Q_{\frac{t}{T}}$ is the empirical quantile function with respect to the $\frac{t}{T}$ percentile. The number of bins T is fixed for the different numerical features. Additionally, the linear layer applies an affine transformation to the input. Formally, for an input vector \mathbf{x} , the output of the Linear layer is computed as $\mathbf{y} = W\mathbf{x} + \mathbf{b}$, where W is a weight matrix, and \mathbf{b} is a bias vector. Intuitively, these embeddings can be seen as an adaptation of One-Hot encoding for numerical features, further enhanced by a linear layer.

• PLR embeddings

These embeddings, inspired by Fourier transformations, were first introduced by (Tancik et al. 2020) and further enhanced by (Gorishniy, Rubachev, and Babenko 2023) for applications on tabular data. A PLR embedding first maps a numerical feature $x^{cont} \in \mathbf{X}^{cont}$ into a $2k$ -dimensional vector using a periodic function, where k is a tunable hyperparameter. Then, a linear layer maps the obtained vector to a d -dimensional vector, where d denotes the dimension of the embedding. Finally, the resulting vector is passed to a ReLU activation function. This process is illustrated in 7 and detailed below:

$$\begin{aligned} \mathbf{z}_i &= f(x_i^{cont}) \\ &= \text{ReLU}(\text{Linear}(\text{Periodic}(x_i^{cont}))) \end{aligned} \quad (5)$$

where

$$\begin{aligned} \text{Periodic}(x) &= \text{concat}[\sin(\mathbf{v}), \cos(\mathbf{v})], \\ \mathbf{v} &= [2\pi c_1 x, \dots, 2\pi c_k x], \end{aligned} \quad (6)$$

and c_i (with $i \in \{1, \dots, k\}$) are trainable parameters. Both embedding dimensions, d and k , are tunable hyperparameters.

The QL embeddings could be viewed as feature encoding since the bins are determined by the distribution of the features in the training set. In contrast, PLR embeddings enable end-to-end training of the c_i parameters through back-propagation. Following the numerical and categorical embeddings, a NN model is used to predict the process building

and sorts as presented in Figure 4. This paper considers MLP and ResNet with and without the embedding layers in the experiments. Additionally, traditional ML methods were used as baselines for comparison with the proposed DL framework. Further details are provided in Section 5.

4.2 Conformal Prediction

As discussed previously, conformal prediction is employed as a post-processing step after training the models for uncertainty quantification of the prediction. Conformal prediction is a model-agnostic and distribution-free method that provides theoretical guarantees on the coverage of the prediction set (Vovk, Gammerman, and Shafer 2005). Instead of making single-point prediction, this approach utilizes a dataset $\mathcal{D}_{calibration}$ (not seen during the training) to calibrate the model output and generate a set of possible outcomes that meet a user-specified target coverage rate. This confidence-aware method is crucial for decision making in load planning, as it assists planners by offering a set of potential processing buildings and sorts, thereby reflecting the inherent prediction uncertainty.

Coverage and *efficiency* are the two key metrics for evaluating uncertainty quantification in the conformal prediction setting. Coverage represents the probability that the true label is included in the prediction set, while efficiency refers to the average size of the prediction set. A model is considered more reliable when it achieves the target coverage with minimal efficiency (i.e., smaller prediction set sizes). To balance these two metrics, this paper employs the Regularized Adaptive Prediction Sets (RAPS) algorithm, which includes a regularization term to penalize large prediction sets (Angelopoulos et al. 2022). Given a trained classification model \hat{f} and a calibration set $\mathcal{D}_{calibration}$, the goal is to learn a function \mathcal{C} that forms prediction sets containing the true label in the test set. More precisely, the goal is to find a function $\mathcal{C}(\cdot)$ that, given an input X_{test} , computes a prediction set $\mathcal{C}(X_{test})$ that contains the ground truth y with a probability satisfying

$$1 - \alpha \leq \mathbb{P}(y \in \mathcal{C}(X_{test})) \quad (7)$$

where $1 - \alpha$ is the desired target coverage with $\alpha \in [0, 1]$.

It is important to note that one can satisfy Equation (7) and reach the target coverage by simply considering a large prediction set size, which is not desirable in practice. Hence, the design of the function \mathcal{C} is crucial for providing high-quality solutions that achieve the target coverage with optimal efficiency (i.e., relatively small average prediction set size). In general, conformal prediction consists of two different steps: 1) the calibration step; and 2) the generation of the prediction sets. (Angelopoulos et al. 2022) proposed the following procedure for these steps, with the calibration step computing an upper probability threshold $\hat{\tau}_{cal}$ and the generation step uses $\hat{\tau}_{cal}$ to compute the prediction set.

During the calibration phase, for each sample $i \in \mathcal{D}_{calibration}$ associated with a feature vector \mathbf{X} , the class labels are sorted from the most probable one to the least probable one according to the output probabilities of the pre-trained model \hat{f} . Then, given that $y \in \mathcal{Y}$ (where $\mathcal{Y} = [1; K]$

and K is the number of classes) is the true label, the following score is calculated as:

$$E_i = \sum_{y'=1}^K \hat{\pi}_x(y') \mathbb{I}_{\{\hat{\pi}_x(y') \geq \hat{\pi}_x(y)\}} + \lambda(o_x(y) - k_{reg})^+ \quad (8)$$

where $\hat{\pi}_x(y')$ is the output probability given by \hat{f} for sample i and class y' , and $o_x(y) = |\{y' \in \mathcal{Y} : \hat{\pi}_x(y') \geq \hat{\pi}_x(y)\}|$ represents the rank of label y among all possible labels, as determined by the probability estimate $\hat{\pi}_x$ (e.g., if y is the third most likely label, $o_x(y) = 3$). The $(\cdot)^+$ operator denotes the positive part. λ and k_{reg} are regularization hyperparameters: k_{reg} is the size of the prediction set from which the algorithm starts penalizing additional labels and λ is the associated penalty factor. More intuitively, E_i corresponds to the cumulative estimated probabilities of the labels until the true label plus a regularization term that penalizes large prediction sets. Based on these calculations, the output $\hat{\tau}_{cal}$ is calculated as the $\lceil (1 - \alpha)(1 + n) \rceil$ largest value in $\{E_i\}_{i=1}^n$ with $n = |\mathcal{D}_{calibration}|$; it can be thought as the score that achieves the target coverage and not more.

At inference time, using $\hat{\tau}_{cal}$ calculated during the calibration step, the goal is to create the prediction set for a sample $j \in \mathcal{D}_{test}$. Without loss of generality, it is assumed that the output labels $\mathcal{Y} = [1; K]$ are sorted from the most to the least probable in terms of estimated probabilities for sample j . Then, the size of the prediction set for sample j is defined as:

$$M = |\{p \in \mathcal{Y} : \sum_{y'=1}^p \hat{\pi}_x(y') + \lambda(j - k_{reg})^+ \leq \hat{\tau}_{cal}\}| + 1 \quad (9)$$

It represents the number of labels to be included in the prediction set, while not exceeded the threshold constraint given by τ_{cal} (the term $+1$ is added to disallow empty prediction sets). The M most probable classes form the $1 - \alpha$ confidence set.

This study uses RAPS as a post-processing step for building and sort predictions (Angelopoulos et al. 2022). The parameters λ and k_{reg} are optimized using an ad-hoc strategy. Specifically, λ is set to 0.001 and k_{reg} to 2, as these values provided a good trade-off between achieving high coverage and maintaining a small average prediction set size.

5 Experimental Details

This section presents the experiments that use the dataset described in Section 3. These experiments compare traditional ML methods with the proposed models. Specifically, the baseline models include Decision Tree (DT), Random Forest (RF), LightGBM (LGBM), CatBoost, and XGBoost. For the DL-based models, both MLP and ResNet architectures are considered. Categorical embeddings are applied in all DL-based experiments, while the performance is evaluated with and without the inclusion of numerical embedding layers.

5.1 Preprocessing

As detailed in Section 3, the dataset consists of numerical, categorical, and temporal features. A preprocessing step is performed before feeding the data into the models as outlined below:

Numerical Features For the traditional ML models, the numerical features are used without any modification. However, for the DL-based models, a Quantile Transformer is used following the addition of noise (distributed as $\mathcal{N}(0, 10^{-5})$) to normalize the data and facilitate the training process.

Categorical Features For traditional ML models (excluding CatBoost), label encoding is applied to features with low cardinality (less than 20 categories). Label encoding assigns a unique integer to each category. Target encoding, which replaces categories with the mean of the target variable, is used for high-cardinality features. CatBoost is trained with its internal encoder for categorical features. For the DL-based models, all categorical features are initially label-encoded and then passed through the categorical embedding layer, as detailed in Section 4.1.

Temporal Features These features, corresponding to the event dates (e.g., scheduled processing date of the load), are first decomposed into day, week, and month components and are label-encoded. Next, given their periodic nature, cyclical encoding is applied to capture continuity (e.g., January is adjacent to December, and Monday is close to Sunday). Each cyclical feature g is represented by two encoded features:

$$g^{sin} = \sin\left(\frac{2\pi g}{\max(g)}\right) \quad (10)$$

$$g^{cos} = \cos\left(\frac{2\pi g}{\max(g)}\right) \quad (11)$$

Following the preprocessing and encoding steps described above, the data is then used as inputs to the models for training.

5.2 Training

Data Split

The experiments are conducted across five distinct time horizons, as shown in Figure 8, to compare models and evaluate their consistency over time. Given the temporal nature of the data, it is first ordered according to the estimated arrival date of the loads and the last month is kept for testing. From the remaining data, 10% is allocated to the calibration set for conformal prediction, 10% to the validation set for hyperparameter, and 80% to the training set. All the experiments are repeated with the same strategy and the average and standard deviation of the metrics are calculated. The results are provided in Section 6.

Hyperparameter tuning

Optuna, an efficient library for hyperparameter tuning (Akiba et al. 2019), is used with 100 trials for the traditional ML models. For the DL-based models, grid search is used. The range of parameters for each model are provided in Appendix A.

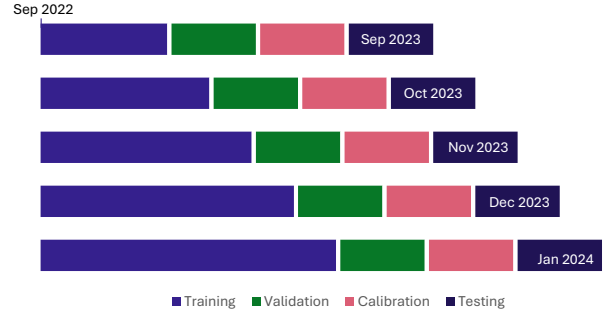


Figure 8: Data splits for experiments : The data was splitted temporally in training, validation, calibration and testing sets. Five experiments were conducted with different testing sets.

Experimental Set up

The experiments are conducted using 1 NVIDIA RTX 6000 GPU and 6 CPUs per task. Each GPU is allocated 16GB of memory. Scikit-Learn (Pedregosa et al. 2018) is used for the implementation and training of the traditional ML models. The training of the DL models is performed using the Adam optimizer and Cross Entropy loss in PyTorch (Paszke et al. 2019). The number of epochs is set to 20 with a patience of 5 across all experiments.

6 Results

This section presents the numerical results comparing different methods as discussed in Section 5. The experiments are conducted across five distinct time horizons with the reported metrics representing mean \pm standard deviation. A detailed explanation of the time horizons is provided in Section 5. Metrics under the 'All Data' category reflect the accuracy across the entire testing dataset, while the 'No Shift', 'Internal Shift', and 'External Shift' categories represent the accuracy specific to each respective shift class.

6.1 Building Prediction

Table 4 presents the performance of different models for building predictions under the first stage of the decision making, which occurs one week ahead of the day of operation. Considering the overall accuracy, XGBoost and RF predict the target processing buildings with more than 99% accuracy. Similarly, the MLP and ResNet models achieve similar performance with the inclusion of the numerical embedding layers. More precisely, the presence of the numerical embedding layers increases the overall accuracy in average by 3.8% and 1.6% for the MLP and ResNet, respectively.

The results for the No Shift and Internal Shift classes show that the XGBoost, RF, and DL-based models with embedding consistently achieve over 99% accuracy.. Similar to the overall accuracy, the effect of the numerical embeddings is evident in enhancing the performance of the DL-based models across these shift classes. The high accuracy in these shift classes is essential for tactical planning, as the majority of the data falls within the No Shift or Internal Shift categories, making a low false alarm rate critical.

Table 4: Comparison of the accuracies for the Building Prediction task: The column labeled 'All Data' represents the accuracies on the complete testing set, while the remaining columns display accuracies based on a partition of the testing set corresponding to different shift classes of the loads.

Model	Num Emb	Building Prediction Accuracy			
		All Data	No Shift	Internal Shift	External Shift
DT	-	0.988 ± 0.003	0.996 ± 0.001	0.994 ± 0.002	0.587 ± 0.031
RF	-	0.990 ± 0.003	0.999 ± 0.001	0.998 ± 0.001	0.502 ± 0.039
CatBoost	-	0.974 ± 0.035	0.982 ± 0.035	0.984 ± 0.032	0.529 ± 0.069
LGBM	-	0.986 ± 0.015	0.995 ± 0.009	0.995 ± 0.008	0.571 ± 0.152
XGBoost	-	0.992 ± 0.001	0.999 ± 0.001	0.998 ± 0.002	0.643 ± 0.030
MLP	✗	0.952 ± 0.075	0.960 ± 0.075	0.959 ± 0.075	0.514 ± 0.068
MLP	PLR	0.990 ± 0.001	0.997 ± 0.001	0.997 ± 0.002	0.592 ± 0.058
MLP	QL	0.990 ± 0.002	0.997 ± 0.001	0.997 ± 0.001	0.622 ± 0.030
ResNet	✗	0.974 ± 0.030	0.983 ± 0.029	0.978 ± 0.037	0.533 ± 0.079
ResNet	PLR	0.989 ± 0.002	0.996 ± 0.001	0.996 ± 0.002	0.590 ± 0.055
ResNet	QL	0.990 ± 0.002	0.997 ± 0.001	0.997 ± 0.001	0.651 ± 0.036

As detailed in Section 3, the dataset exhibits a significant class imbalance, with External Shifts comprising only 2% of the dataset. This imbalance presents a key challenge: maximizing overall accuracy across the entire test set while effectively predicting External Shifts, where the processing building differs from the intended one. This is critical for tactical load-planning where the loads are supposed to be re-routed into another building in advance. The results in Table 4 under the 'External Shifts' sub-column indicate that all models achieve accuracy between 50% and 65% in predicting the correct buildings within this challenging class. Among them, ResNet-QL outperforms all other models in this subclass, surpassing XGBoost. Additionally, the importance of numerical embedding is evident, with accuracy improvements of 11% and 12% for MLP and ResNet, respectively.

Additionally, although not explicitly presented in Table 4, an intriguing observation is the remarkably low number of misclassifications between distinct clusters in the building prediction task. Specifically, less than 0.1% of the loads that were processed in Cluster 1 are incorrectly predicted to be processed in Cluster 2, or vice versa. This finding highlights the model ability to accurately capture the interactions within clusters, which is crucial for tactical planning, ensuring that loads are not mistakenly shifted to buildings in a different cluster than originally planned.

6.2 Sort Prediction and Importance of Two-Stage Decision Making

Table 5 illustrates the performance of the different models on the prediction of the sort, one week before the day of operations (i.e., stage one of the prediction). While all the models achieve a global accuracy higher than 80%, some

achieve significantly higher performance such as ResNet-QL, ResNet-PLR, MLP-PLR that achieve accuracies exceeding 86%, slightly outperforming state of the art traditional models like XGBoost and LightGBM.

As detailed in Section 2, the processing sort can differ from the planned processing sort in both Internal Shifts and External Shifts. Table 5 reports the conditional accuracies across the different shift classes. The accuracy of all models for sort prediction under the No Shift class is above 90% (with the exception of DT with 88% accuracy), which demonstrates the reliability of the models in predicting the sorts with low false positive errors in this class. However, the accuracy drops significantly for the sort prediction in the Internal Shift and External Shift sub-classes, ranging between 50% and 60%. This reduction is primarily due to the lack of crucial features necessary for the sort prediction one week before the day of operations.

Even if the initial stage does not yield optimal performance, it is important for the planners to have an estimate of the network and load volumes at each building-sort pair one week before the operations. This early insight helps to identify potential load shifts and ensures better allocation of personnel and equipment across sorts.

The results for the sort prediction on the day of operation after incorporating the estimated arrival time of the loads as an additional feature (i.e., second stage of the decision-making) are presented in Table 6. A comparison of the results in Table 5 and 6 shows that the inclusion of the additional feature results in a consistent improvement of approximately 5-6% of the overall accuracy across various models. Moreover, it is noteworthy that the Internal Shift and External Shift sub-classes exhibit a significant improvement of around 20% across different models.

Table 5: Comparison of the accuracies for the Sort Prediction task one week before the day of operations: The column labeled 'All Data' represents the accuracies on the complete testing set, while the remaining columns display accuracies based on a partition of the testing set corresponding to different shift classes of the loads.

Model	Num Emb	Sort Prediction Accuracy - Week ahead			
		All Data	No Shift	Internal Shift	External Shift
DT	-	0.801 ± 0.058	0.888 ± 0.078	0.459 ± 0.032	0.490 ± 0.050
RF	-	0.824 ± 0.055	0.920 ± 0.080	0.449 ± 0.029	0.535 ± 0.048
CatBoost	-	0.812 ± 0.058	0.903 ± 0.079	0.447 ± 0.043	0.542 ± 0.066
LGBM	-	0.860 ± 0.016	0.947 ± 0.017	0.518 ± 0.039	0.587 ± 0.082
XGBoost	-	0.862 ± 0.013	0.944 ± 0.012	0.533 ± 0.035	0.598 ± 0.096
MLP	✗	0.838 ± 0.032	0.917 ± 0.033	0.520 ± 0.038	0.569 ± 0.088
MLP	PLR	0.864 ± 0.015	0.954 ± 0.008	0.500 ± 0.019	0.613 ± 0.055
MLP	QL	0.853 ± 0.014	0.936 ± 0.011	0.520 ± 0.021	0.587 ± 0.044
ResNet	✗	0.844 ± 0.034	0.926 ± 0.031	0.510 ± 0.043	0.568 ± 0.058
ResNet	PLR	0.866 ± 0.014	0.953 ± 0.011	0.519 ± 0.032	0.564 ± 0.067
ResNet	QL	0.865 ± 0.012	0.953 ± 0.006	0.508 ± 0.027	0.593 ± 0.061

Table 6: Comparison of the accuracies for the Sort Prediction task on the day of operations: The column labeled 'All Data' represents the accuracies on the complete testing set, while the remaining columns display accuracies based on a partition of the testing set corresponding to different shift classes of the loads.

Model	Num Emb	Sort Prediction Accuracy - Day of Operations			
		All Data	No Shift	Internal Shift	External Shift
DT	-	0.851 ± 0.074	0.902 ± 0.083	0.648 ± 0.073	0.672 ± 0.131
RF	-	0.861 ± 0.079	0.910 ± 0.086	0.671 ± 0.079	0.670 ± 0.125
CatBoost	-	0.864 ± 0.077	0.909 ± 0.081	0.679 ± 0.088	0.712 ± 0.123
LGBM	-	0.922 ± 0.007	0.961 ± 0.006	0.770 ± 0.027	0.776 ± 0.036
XGBoost	-	0.925 ± 0.007	0.963 ± 0.004	0.772 ± 0.021	0.783 ± 0.038
MLP	✗	0.908 ± 0.022	0.951 ± 0.011	0.734 ± 0.072	0.763 ± 0.057
MLP	PLR	0.917 ± 0.009	0.957 ± 0.005	0.751 ± 0.025	0.782 ± 0.053
MLP	QL	0.916 ± 0.008	0.957 ± 0.004	0.755 ± 0.033	0.751 ± 0.056
ResNet	✗	0.912 ± 0.033	0.958 ± 0.010	0.735 ± 0.042	0.750 ± 0.071
ResNet	PLR	0.922 ± 0.010	0.958 ± 0.013	0.750 ± 0.039	0.764 ± 0.051
ResNet	QL	0.916 ± 0.014	0.957 ± 0.014	0.754 ± 0.035	0.781 ± 0.042

6.3 Conformal Prediction

As detailed in Section 4.2, conformal prediction is incorporated into each model within the proposed framework. This approach enables the models to generate prediction sets containing multiple buildings or sorts, rather than making a single prediction. This sub-section presents the results in terms of coverage and efficiency for each model, showing that models reach the target coverage, while producing typ-

ically small prediction sets.

The target coverage is set to 99% (i.e., $\alpha = 0.01$) for the building prediction task due to 1) its significant impact on the tactical planning, and 2) the existing class imbalance in the data which only includes 2% of the data from the External Shift Class. For the sort prediction, the target coverage is set to 95% (i.e., $\alpha = 0.05$).

For the building prediction task, the coverage and effi-

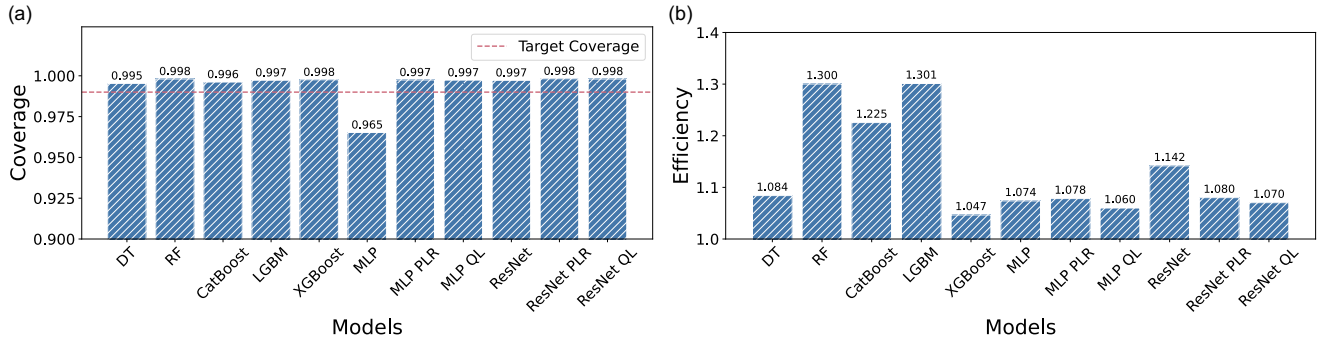


Figure 9: Efficiency and coverage per model for the 6-class Building Prediction task: (a) shows the coverage and the fixed target coverage for the building prediction task across the different models. (b) shows the efficiency (average size of the prediction sets) for different models for the building prediction.

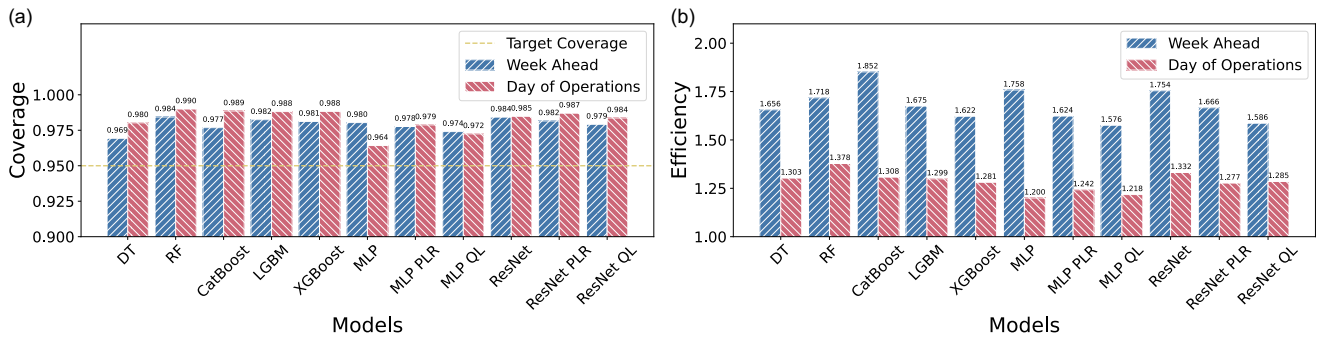


Figure 10: Efficiency and coverage per model for the 3-class Sort Prediction task : (a) shows the coverage and the fixed target coverage for the sort prediction task across the different models. (b) shows the efficiency (average size of the prediction sets) for different models for the sort prediction. The blue bar corresponds to the metrics obtained one week before the day of operations and the red one is the one obtained on the day of operations.

ciency of different models are presented in Figure 9. All models reach the target coverage with empirical coverage ranging from 99.5% to 99.8%, except for the regular MLP model (with no numerical embedding). This can be attributed to the inherent weakness of the MLP model in this prediction task, resulting in inadequate probability calibration using the calibration data, and insufficient coverage.

Comparing the efficiency of the models on Figure 9 reveals that XGBoost achieves the lowest average prediction set size (i.e., efficiency). The proposed DL-based models (with the inclusion of numerical embeddings) also achieve a competitive efficiency ranging between 1.08 to 1.06.

Figures 10 presents the efficiency and coverage for sort prediction for each model, both one week ahead and on the day of operations. Notably, all models meet the target coverage for sort prediction. Additionally, the models' confidence improves significantly from the week-ahead prediction to the day of operations, as evidenced by the decrease in efficiency (i.e., reduction in the average prediction set size). This highlights the effectiveness of the two-stage decision-making process and the importance of load arrival times in accurately predicting the processing sorts.

Adaptativeness Property

As detailed in Section 4.2, this study employs RAPS as the scoring method for the uncertainty quantification. A key feature of RAPS is its adaptive nature, which adjusts prediction set sizes based on the complexity of the samples. This adaptability ensures that difficult-to-classify samples achieve higher efficiency without significantly compromising the conditional coverage.

Figure 11 illustrates the conditional efficiency across different shift classes for the three tasks under consideration using the ResNet-QL model (similar results are obtained for the other methods, however, they are omitted here for simplicity). In the case of Building Prediction, the conditional efficiency nearly doubles for samples experiencing external shifts, indicating that the model effectively captures the complexity of these samples, where the planned processing building differs from the actual processing building. For Sort Prediction, conditional efficiency increases by approximately 7% between No Shift and Internal Shifts, and by around 11% from Internal Shifts to External Shifts. This trend underscores the model ability to accommodate the growing complexity associated with accurate predictions for shifted loads.

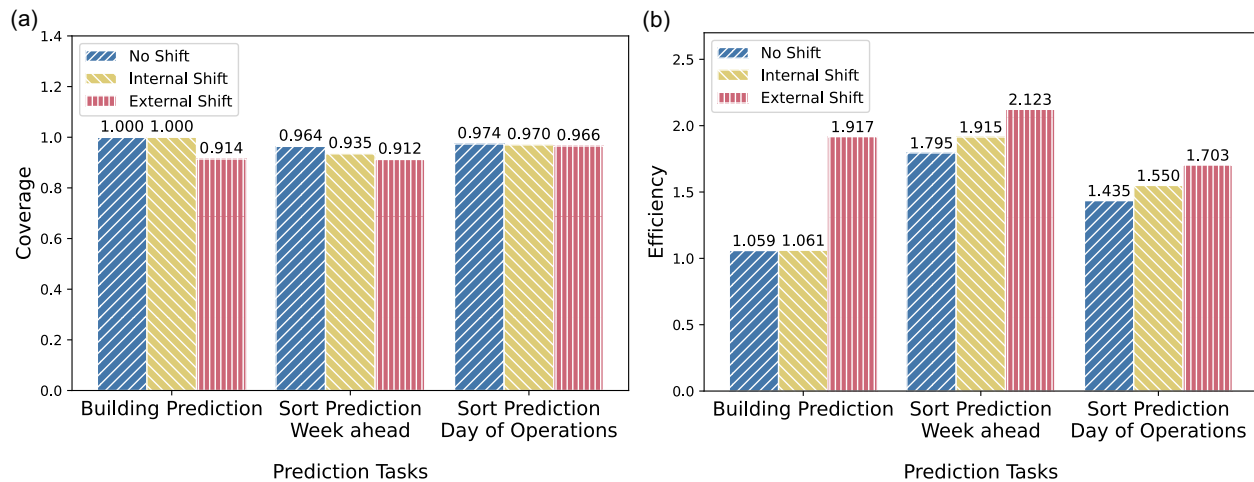


Figure 11: Conditional efficiency and coverage for the three different tasks using ResNet-QL: Building Prediction, Sort Prediction - Week ahead, and Sort Prediction - Day of operations. The metrics are illustrated across a partition of the data: No Shift, Internal Shift, and External Shift.

Figure 11 presents the corresponding conditional coverages. For Building Prediction, loads from External Shift class are predicted with a conditional coverage of 0.914, demonstrating that the model effectively manages to maintain high coverage, thus supporting accurate shifting decisions. Similar patterns are observed for sort predictions. Notably, the target coverage (set at 0.95) is consistently met across all shift classes for predictions made on the day of operations.

7 Conclusion and Future Research

This paper introduced a novel DL-based framework using a two-stage decision-making to effectively address the inbound load shifting problem. The experimental results demonstrated the efficacy of the proposed method in accurately predicting the processing building and sorts across both majority and minority classes. By leveraging the theoretical guarantees and enhanced interpretability of conformal prediction, the proposed framework offers valuable support for planners in developing effective inbound load plans for both tactical and operational contexts. Unlike current practices that often rely on partial network views, the proposed method utilizes historical data to guide decision making, ensuring more informed and sensible choices. Additionally, its scalability allows network integration, enhancing the learning process and improving decision alignment.

The findings highlight the importance of a two-stage decision-making process for sort prediction. Notably, the results showed an improvement of around 20% in accuracy between predictions made one week before the day of operations and on the day of operations for Internal and External Shift sub-classes across various models. Additionally, the second stage of the decision-making process yielded more confident predictions, highlighting the critical role of load arrival time in accurately predicting processing sorts.

The proposed DL-based models showed performance

comparable to XGBoost, widely regarded as state of the art on tabular data analysis. Additionally, the results highlighted the importance and effectiveness of the embedding layers in enhancing the performance of the DL-based models. While tuning the parameters of the embedding layers can introduce challenges during training, the proposed DL architecture supports transfer learning, allowing for domain adaptation by using pre-trained models as a warm start. Moreover, the DL-based model enables the integration of customized loss functions that account for decision-associated costs.

Future research will focus on integrating the DL model with an optimization framework to account for decision-associated costs, including end-to-end training for more optimized decision making. Additionally, group-conditional conformal prediction will be explored to enhance the robustness of predictions for minority classes.

References

- Akiba, T.; Sano, S.; Yanase, T.; Ohta, T.; and Koyama, M. 2019. Optuna: A Next-generation Hyperparameter Optimization Framework. arXiv:1907.10902.
- Angelopoulos, A.; Bates, S.; Malik, J.; and Jordan, M. I. 2022. Uncertainty Sets for Image Classifiers using Conformal Prediction. arXiv:2009.14193.
- Associations, A. T. 2023. Economics and Industry Data.
- Bakir, I.; Erera, A.; and Savelsbergh, M. 2021. *Motor Carrier Service Network Design*, 427–467. Cham: Springer International Publishing. ISBN 978-3-030-64018-7.
- Baubaid, A.; Boland, N.; and Savelsbergh, M. 2018. Dealing with Demand Uncertainty in Service Network and Load Plan Design. 63–71. ISBN 978-3-319-93030-5.
- Boland, N.; Hewitt, M.; Marshall, L.; and Savelsbergh, M. 2017. The Continuous-Time Service Network Design Problem. *Operations Research*, 65(5): 1303–1321.

- Bugow, S.; and Kellenbrink, C. 2023. The parcel hub scheduling problem with limited conveyor capacity and controllable unloading speeds. *OR Spectrum*, 45: 1–33.
- Crainic, T. G. 2000a. Service network design in freight transportation. *European journal of operational research*, 122(2): 272–288.
- Crainic, T. G. 2000b. Service network design in freight transportation. *European Journal of Operational Research*, 122(2): 272–288.
- Eskandarzadeh, S.; and Fahimnia, B. 2024. Containerised parcel delivery: Modelling and performance evaluation. *Transportation Research Part E: Logistics and Transportation Review*, 186: 103519.
- Gorishniy, Y.; Rubachev, I.; and Babenko, A. 2023. On Embeddings for Numerical Features in Tabular Deep Learning. arXiv:2203.05556.
- Herszterg, I.; Ridouane, Y.; Boland, N.; Erera, A.; and Savelsbergh, M. 2022. Near real-time loadplan adjustments for less-than-truckload carriers. *European Journal of Operational Research*, 301(3): 1021–1034.
- Hewitt, M. 2019. Enhanced Dynamic Discretization Discovery for the Continuous Time Load Plan Design Problem. *Transportation Science*, 53(6): 1731–1750.
- James C. Chen, D. A.; and Chen, T.-L. 2024. Current research and future challenges in parcel hub towards logistics 4.0: a systematic literature review from a decision-making perspective. *International Journal of Production Research*, 0(0): 1–32.
- Lindsey, K.; Erera, A.; and Savelsbergh, M. 2016. Improved integer programming-based neighborhood search for less-than-truckload load plan design. *Transportation science*, 50(4): 1360–1379.
- McWilliams, D. L. 2009. A dynamic load-balancing scheme for the parcel hub-scheduling problem. *Computers & Industrial Engineering*, 57(3): 958–962.
- Mikolov, T.; Chen, K.; Corrado, G.; and Dean, J. 2013. Efficient Estimation of Word Representations in Vector Space. arXiv:1301.3781.
- Munkhdalai, L.; Park, K. H.; Batbaatar, E.; Theera-Umpon, N.; and Ryu, K. 2020. Deep Learning-Based Demand Forecasting for Korean Postal Delivery Service. *IEEE Access*, 8: 188135–188145.
- Ojha, R.; Chen, W.; Zhang, H.; Khir, R.; Erera, A.; and Hentenryck, P. V. 2024. Optimization-based Learning for Dynamic Load Planning in Trucking Service Networks. arXiv:2307.04050.
- Paszke, A.; Gross, S.; Massa, F.; Lerer, A.; Bradbury, J.; Chanan, G.; Killeen, T.; Lin, Z.; Gimelshein, N.; Antiga, L.; Desmaison, A.; Köpf, A.; Yang, E.; DeVito, Z.; Raison, M.; Tejani, A.; Chilamkurthy, S.; Steiner, B.; Fang, L.; Bai, J.; and Chintala, S. 2019. PyTorch: An Imperative Style, High-Performance Deep Learning Library. arXiv:1912.01703.
- Pedregosa, F.; Varoquaux, G.; Gramfort, A.; Michel, V.; Thirion, B.; Grisel, O.; Blondel, M.; Müller, A.; Nothman, J.; Louppe, G.; Prettenhofer, P.; Weiss, R.; Dubourg, V.; Vanderplas, J.; Passos, A.; Cournapeau, D.; Brucher, M.; Perrot, M.; and Édouard Duchesnay. 2018. Scikit-learn: Machine Learning in Python. arXiv:1201.0490.
- Romano, Y.; Sesia, M.; and Candès, E. J. 2020. Classification with Valid and Adaptive Coverage. arXiv:2006.02544.
- Tancik, M.; Srinivasan, P. P.; Mildenhall, B.; Fridovich-Keil, S.; Raghavan, N.; Singhal, U.; Ramamoorthi, R.; Barron, J. T.; and Ng, R. 2020. Fourier Features Let Networks Learn High Frequency Functions in Low Dimensional Domains. arXiv:2006.10739.
- Tsolaki, K.; Vafeiadis, T.; Nizamis, A.; Ioannidis, D.; and Tzovaras, D. 2023. Utilizing machine learning on freight transportation and logistics applications: A review. *ICT Express*, 9(3): 284–295.
- U.S. Department of Transportation, B. o. T. S. 2014. U.S. Freight on the Move: Highlights From the 2012 Commodity Flow Survey Preliminary Data.
- Vovk, V.; Gammerman, A.; and Shafer, G. 2005. *Algorithmic Learning in a Random World*. Berlin, Heidelberg: Springer-Verlag. ISBN 0387001522.
- Wieberneit, N. 2007. Service network design for freight transportation: a review. *OR Spectrum*, 30: 77–112.
- Yan, H.; Tan, H.; Wang, H.; Zhang, D.; and Yang, Y. 2024. Robust Route Planning under Uncertain Pickup Requests for Last-mile Delivery. In *Proceedings of the ACM Web Conference 2024, WWW '24*, 3022–3030. New York, NY, USA: Association for Computing Machinery. ISBN 9798400701719.
- Ye, L.; Zhou, J.; Yin, Z.; Han, K.; Hu, H.; and Song, D. 2024. *A Novel Hybrid Graph Learning Method for Inbound Parcel Volume Forecasting in Logistics System*, 352–360.

A Appendix

Table 7: Tuned Parameters and Ranges for XGBoost and LightGBM

Parameter	Range
max depth	[2, 10]
learning rate	[1e-5, 1.0] (log scale)
n estimators	[50, 500]
min child weight	[1, 10]
alpha	[1e-8, 1.0] (log scale)
gamma	[1e-8, 1.0] (log scale)
subsample	[0.5, 1.0] (log scale)
colsample bytree	[0.01, 1.0] (log scale)
reg alpha	[1e-8, 1.0] (log scale)
reg lambda	[1e-8, 1.0] (log scale)

Table 8: Tuned Parameters and Ranges for CatBoost

Parameter	Range
learning rate	[1e-5, 1.0] (log scale)
colsample bylevel	[0.05, 1]
depth	[2, 10]
min data in leaf	[1, 100]

Table 9: Tuned Parameters and Ranges for Random Forest

Parameter	Range
n estimators	[50, 500]
max depth	[2, 10]
min samples split	[2, 30]
min samples leaf	[1, 30]
max features	[0.001, 1]

Table 10: Tuned Parameters and Ranges for Decision Tree

Parameter	Range
max depth	[1, 100]
min samples split	[2, 30]
min samples leaf	[1, 30]

Table 11: Tuned Parameters and Ranges for MLP and ResNet

Parameter	Range
n blocks	[2, 10]
d block	[64, 256]